Imaging direct, dynamin-dependent recapture of fusing secretory granules on plasma membrane lawns from PC12 cells

Phillip Holroyd*†, Thorsten Lang*†, Dirk Wenzel*, Pietro De Camilli‡, and Reinhard Jahn*§

*Department of Neurobiology, Max Planck Institute for Biophysical Chemistry, 37077 Göttingen, Germany; and ‡Department of Cell Biology and Howard Hughes Medical Institute, Yale University School of Medicine, New Haven, CT 06510

Contributed by Pietro De Camilli, November 7, 2002

During exocytosis, secretory granules fuse with the plasma membrane and discharge their content into the extracellular space. The exocytosed membrane is then reinternalized in a coordinated fashion. A role of clathrin-coated vesicles in this process is well established, whereas the involvement of a direct retrieval mechanism (often called kiss and run) is still debated. Here we report that a significant population of docked secretory granules in the neuroendocrine cell line PC12 fuses with the plasma membrane, takes up fluid-phase markers, and is retrieved at the same position. Fusion allows for complete discharge of small molecules, whereas GFP-labeled neuropeptide Y (molecular mass ≈35 kDa) is only partially released. Retrieved granules were preferentially associated with dynamin. Furthermore, recapture is inhibited by guanosine 5′-[γ-thio]triphosphate and peptides known to block dynamin function. We conclude that secretory granules can be recaptured immediately after formation of an exocytotic opening by an endocytic reaction that is spatially and temporally coupled to soluble *N*-ethylmaleimide-sensitive factor attachment protein receptor (SNARE)-dependent fusion, but is not a reversal of the fusion reaction.

Neurons and neuroendocrine cells release hormones and neurotransmitters by Ca^{2+}-dependent exocytosis from storage vesicles (1). One class of vesicles, synaptic vesicles, consists of small vesicles that store nonpeptide neurotransmitters. Another class, secretory granules or large dense core vesicles, contains peptide neurotransmitters and may also contain amines and other nonpeptide neurotransmitters (2). After exocytosis, the membrane of the fusing vesicles is recovered by endocytosis, thus maintaining a net equilibrium between membrane addition and membrane removal. The precise mechanism of membrane recapture from the plasma membrane remains controversial. One major and well documented pathway involves recovery by clathrin-mediated endocytosis after the collapse of the newly fused membrane and its full integration in the plasma membrane (3). Another pathway involves the rapid closure of the exocytotic fusion pore so that the vesicle integrity is maintained during the exo–endocytic reaction (4, 5). Evidence for this pathway comes from biophysical studies of secretion from large vesicles such as dense core vesicles of neuroendocrine cells and secretory granules of mast cells. These studies demonstrated "flickering" of the fusion pore and reclosure without full fusion (6, 7). In addition, studies of mast cells (8) and endocrine cells (9, 10) showed that stepwise rises in capacitance caused by fusion of individual vesicles were often balanced by step decreases that were interpreted as endocytic reversion of the fusion event. However, in these studies it has often remained unclear whether the rapid endocytosis of endocrine secretory granules represents recapture of an incompletely fused vesicle or whether the vesicle fuses completely with the plasma membrane and is then retrieved in a coupled but mechanistically independent and separate step.

Vesicular transport in the secretory pathway can be broken down into elementary steps that occur in many variations in every eukaryotic cell but whose general characteristic is vectoriality. Vesicles are formed by membrane budding from a precursor membrane. They are then transported to their destination, where they dock and fuse with the target membrane. Forward vesicle traffic is balanced by compensatory retrograde vesicle traffic. These steps are biologically irreversible, a prerequisite for ordered and directed transport. Accordingly, the molecular machines for budding and fusion, at least as far as they are understood, appear to be completely different. Fusion is mediated by evolutionarily conserved proteins including soluble *N*-ethylmaleimide-sensitive factor attachment protein receptors (SNAREs), Rabs, and Sec1/Munc18-related proteins (11, 12). In contrast, budding and fission, i.e., the reversal of vesicle fusion, normally involves the formation of specialized protein coats and, at least in the case of budding from the cell surface, a fission machinery (13). A rapidly reversible fusion event raises the interesting question of whether this process is mediated by a reversibility of the reactions involved in fusion or by two sequential and different reactions occurring in rapid sequence.

We have now used fluorescence microscopy on PC12 plasma membrane lawns and electron microscopy on intact PC12 cells to study the recapture of large dense core vesicles after stimulation of exocytosis. We demonstrate the occurrence of direct granule reuptake and the dynamin dependence of this process. While this study was in progress, Graham *et al.* (14) reported a dynamin-dependent rapid reclosure of putative exocytotic fusion pores in chromaffin cells based on amperometric studies of amine release. The two studies complement each other in demonstrating that secretory granules can be recaptured without full collapse into the membrane at the site of exocytosis, but that closure of the fusion pore does not simply represent a reversal of the fusion reaction.

Materials and Methods

Cell Culture, Transfection, Immunostaining, and Preparation of Recombinant Amphiphysin. PC12 cells clone 251 (15) were maintained and propagated as described (16). Transfection of PC12 cells with neuropeptide Y (NPY)-GFP [NPY fused to the N-terminal end of enhanced GFP (CLONTECH)] was performed essentially as described (17). For immunostaining, a rabbit polyclonal serum raised against residues 2–17 of rat dynamin 1 was obtained from Synaptic Systems (Göttingen, Germany). As secondary antibody, Cy5-coupled goat anti-rabbit (Dianova, Hamburg, Germany) was used. GST-tagged amphiphysin was prepared as described (18).

Preparation of Membrane Sheets and *in Vitro* Exocytosis Assay. Membrane sheets were prepared as described (19) in ice-cold sonication buffer (20 mM Hepes, pH 7.2/120 mM potassium glutamate/20 mM potassium acetate/10 mM EGTA/2 mM

Abbreviations: NPY, neuropeptide Y; HRP, horseradish peroxidase.

†P.H. and T.L. contributed equally to this work.

§To whom correspondence should be addressed. E-mail: rjahn@gwdg.de.

 www.pnas.org/cgi/doi/10.1073/pnas.222677399

MgATP/0.5 mM DTT) and incubated at room temperature for 10 min (in the presence/absence of various inhibitors/peptides where indicated) during which a sheet with 15 or more brightly fluorescent granules was located. Suitable preparations were then stimulated by using the indicated $[Ca^{2+}]_{free}$ in the presence of 2 mM MgATP, 0.5 mg/ml rat brain cytosol (19), omitted in the experiments shown in Fig. 2*D*, and 5 μM sulforhodamine 101 (Molecular Probes). Membrane sheets were imaged every 30 s for 15 min then washed twice for 5 min with potassium glutamate buffer (20 mM Hepes, pH 7.2/120 mM potassium glutamate/20 mM potassium acetate) to remove excess sulforhodamine 101. Membranes were visualized by using 1-(4-trimethylammonium)-6-phenyl-1,3,5-hexatriene (Molecular Probes); 0.1 and 0.5 μM $[Ca^{2+}]_{free}$ were buffered by using 10 mM EGTA, whereas 1.5, 10, and 50 μM $[Ca^{2+}]_{free}$ buffers used 10 mM 1,3-diamino-2-propanol-*N*,*N*,*N*′,*N*′-tetraacetic acid (DPTA). EGTA and DPTA calcium buffers were calibrated against $CaCl_2/MgCl_2$ solutions of known concentration by using fura-2 or mag-fura-2 (Molecular Probes) ratiometric dyes, respectively. In some experiments, PC12 cells were prestimulated for 2 min by high K^+ Ringer's buffer (50 mM NaCl/80 mM KCl/5 mM $CaCl_2$/1 mM $MgCl_2$/48 mM glucose/10 mM Hepes-NaOH, pH 7.4) at 37°C in the presence of 20 μM sulforhodamine 101 before membrane sheet preparation. In control experiments KCl was reduced to 4 mM and NaCl was elevated to 130 mM (low K^+ Ringer's buffer). Fluorescence microscopy was performed as described (20). The focal position was controlled by using a low-voltage piezo translater driver and a linear variable transformer displacement sensor/controller (Physik Instrumente, Waldbronn, Germany). Fluorescence filters used were: GFP Zeiss filter set 10 (excitation BP 450–490, BS 510, emission BP 515–565), acridine orange Zeiss filter set 09 (as Zeiss 10 but emission LP 520), Cy3 Zeiss filter set 15 (excitation BP 540–552, BS 580, emission LP 590), Cy5 Chroma Technology (Brattleboro, VT) filter set HQ41008 (excitation BP 590–650, BS 660, emission BP 662–738), and TMA-DPH Zeiss filter set 02 (excitation G 365, BS 395, emission LP 420). All images were analyzed with METAMORPH software (Universal Imaging, Media, PA). Granule intensities and positions were traced between successive frames by using circles with a diameter of 10 pixels.

Uptake of Horseradish Peroxidase (HRP) and Electron Microscopy. PC12 cells (maintained as described) were washed twice in prewarmed K-PBS (2.7 mM KCl/1.5 mM KH_2PO_4/137 mM NaCl/8 mM Na_2HPO_4, pH 7.3), followed by a 2-min stimulation in high K^+ Ringer's buffer with 1 mg/ml HRP (EC 1.11.1.7) at 37°C. Cells were then washed twice with K-PBS. Ultrathin cryo-sections were prepared as described (17), but before sucrose infusion diaminobenzidine (DAB) labeling was performed. Blocks were incubated with 1 mg/ml DAB and 0.01% H_2O_2 in TBS (20 mM Tris, pH 7.4/150 mM NaCl) for 1 h at room temperature. ImmunoGold labeling of cryo-sections was performed as described (17) with a 1:40 dilution of a polyclonal anti-GFP antibody.

Results

Transient Exocytosis of Secretory Granules in a Cell-Free Preparation. We had characterized exocytosis in a cell-free preparation (19). PC12 cells are grown on glass coverslips and disrupted by a brief ultrasound pulse, leaving a glass-adhered plasma membrane sheet with up to 100 (usually 20–50) attached secretory granules. Addition of calcium, cytosol, and MgATP leads to exocytosis of secretory granules, which proceeds at a constant rate over a time course of 15 min. Fusion events can be monitored by the loss of the acidophilic fluorescent dye acridine orange (19), which uniformly results in the abrupt disappearance of individual granules (see F_{lost} in Fig. 1*A*).

When NPY-GFP (17) instead of acridine orange was used as content marker for secretory granules, a surprising pattern of fluorescence intensity changes was observed (Fig. 1 *A* and *B*). In addition to abrupt loss of fluorescence intensity (F_{lost}), we

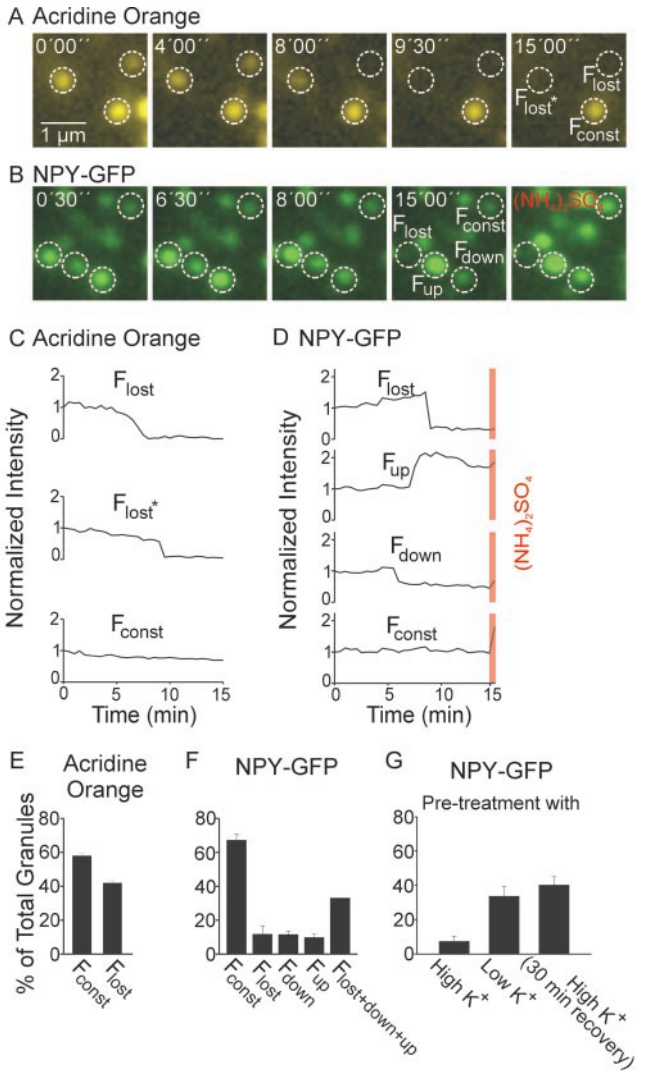

Fig. 1. Ca^{2+}-dependent exocytosis of secretory granules in a cell-free preparation, monitored by video microscopy using either acridine orange or NPY-GFP as content marker. Membrane sheets with attached secretory granules labeled by either the acidophilic dye acridine orange (*A*) or expression of the secretory granule marker NPY-GFP (*B*) were incubated in a solution containing 500 nM free calcium, 0.5 mg/ml rat brain cytosol, and 2 mM MgATP to stimulate exocytosis. Images were taken every 30 s for 15 min, and the fluorescence intensity of individual granules was measured (see *Materials and Methods*). (*C* and *D*) Exemplary intensity traces of those granules shown in *A* and *B*. Intensity values were corrected for local background, normalized to initial intensity, and plotted against time. (*C*) When acridine orange was used, granules either lost their fluorescence (F_{lost}) or were slowly bleached (F_{const}). (*D*) Changes in fluorescence intensity of granules labeled with NPY-GFP. Granules disappeared (F_{lost}), became brighter (F_{up}), became dimmer (F_{down}), or did not change in fluorescence intensity (F_{const}). Orange bars, fluorescence intensity after addition of 20 mM $(NH_4)_2SO_4$ that abolishes the pH gradient across the granule membrane. (*E* and *F*) Relative abundance (percent of total) of granules classified according to their fluorescence intensity changes as described above. For acridine orange four membrane sheets were analyzed, and for NPY-GFP 10 membrane sheets were analyzed. (*G*) Exocytosis of NPY-GFP-labeled secretory granules from membrane sheets derived from intact cells pretreated with high K^+ or control buffers for 2 min at 37°C in the presence of 20 μM sulforhodamine. Membrane sheets were prepared immediately after such treatment or after a 30-min recovery at 37°C. Membrane sheets were then stimulated as described above. Values are mean ± SEM.

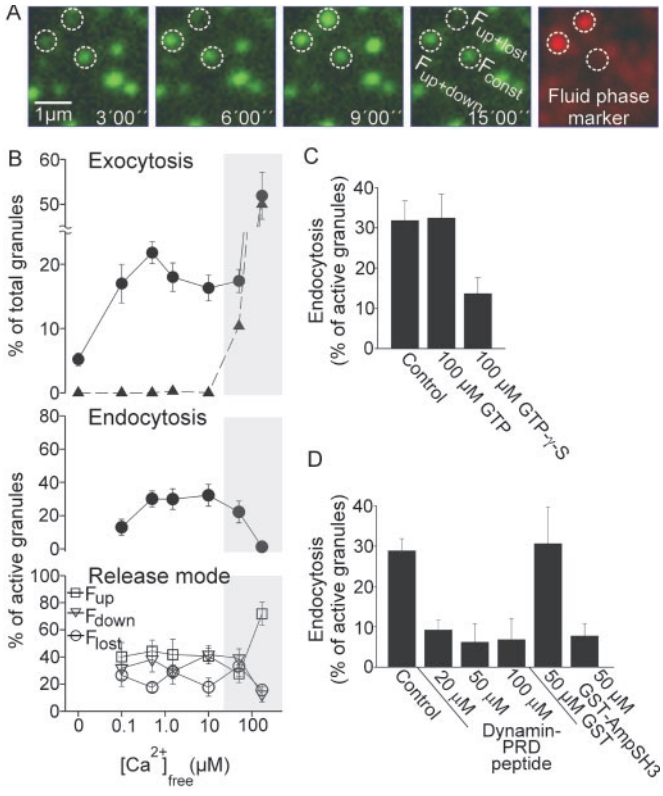

Fig. 2. Endocytic capture of the fluid-phase marker sulforhodamine by secretory granules after stimulation of exocytosis and its dependence on calcium. (*A*) Membrane sheets with docked NPY-GFP-labeled secretory granules were stimulated for exocytosis (as in Fig. 1) in the presence of 5 μM sulforhodamine and imaged as before. Exemplary images from the sequence in the GFP channel are shown. After 15 min, sulforhodamine was washed out, and images were acquired in the red and the green channel. Two red spots are visible that are concentric with secretory granules that have undergone exocytosis ($F_{up+lost}$ and $F_{up+down}$ in *A*), whereas an inactive granule (F_{const} in *A*) has no corresponding signal. (*B*) Calcium dependence of exocytosis, endocytosis, and the individual release modes. For each calcium concentration, five to nine membrane sheets were analyzed. Rates of endocytosis were corrected for random overlap (ranging between 3% and 5%) as described (20). The shaded area indicates calcium concentrations at which the assay allows no evaluation of the data because secretory granules not associated with the membrane sheets but attached to the glass also display changes in fluorescence intensity (triangles, *Upper*). Values are mean ± SEM. Effect of (*C*) GTP and GTPγS or (*D*) a peptide corresponding to the proline-rich domain of dynamin (dynamin PRD peptide) and a GST fusion protein corresponding to the Src homology 3 domain of amphiphysin on endocytosis of secretory granules. Note that experiments shown in *D* were performed in the absence of cytosol to avoid interference with cytosolic proteins. Values are mean ± SEM (n = 6–11 membrane sheets for each condition).

observed dimming (F_{down}) and also brightening (F_{up}) of secretory granules (Fig. 1 *B* and *D*). Occasionally, granules were observed that underwent consecutively brightening and dimming or loss (see, e.g., Fig. 2*A*). All changes in fluorescence intensity depended on calcium, and there was no strong preference for one or the other mode over a broad range of calcium concentrations (Fig. 1*F*, see also Fig. 2*B Lower*). In addition, there was no correlation between changes in fluorescence and the initial fluorescence intensity of a granule (data not shown).

GFP fluorescence is reduced in intensity by 50% when the pH is shifted from 7.5 to 5.5 (21). Thus, the increase in fluorescence intensity may be caused by an alkalinization of the acidic granule interior. To test for this possibility, we added $(NH_4)_2SO_4$ that neutralizes the pH gradient across the vesicle membrane. Indeed, granules that did not exhibit a fluorescence intensity change during stimulation (F_{const}) increased 72 ± 7% (n = 134 granules) in intensity (Fig. 1*D*). F_{up} granules also increased in brightness but to a lesser extent (22 ± 5%, n = 44 granules), and there was a significant fraction in which no increase was observed after addition of $(NH_4)_2SO_4$. F_{down} granules also showed an increase (46 ± 10%, n = 18 granules). Control experiments showed that $(NH_4)_2SO_4$ has no direct effect on GFP fluorescence (data not shown).

These data can be best explained by a transient fusion of secretory granules, followed by recapture of the secretory granule at the site of exocytosis. The increase in fluorescence (F_{up}) is probably caused by vesicles that had undergone transient fusion for a period sufficient for content neutralization because of exposure to extracellular buffer but not sufficient for NPY-GFP to escape. That such events are transient is further supported by the observation that some F_{up} granules are capable of reacidification as shown by a slow decrease in their intensity after fusion (see F_{up} granule in Fig. 1*D*), which can be reversed by the addition of $(NH_4)_2SO_4$.

If secretory granules indeed undergo transient fusion, their interiors are expected to be temporarily accessible to extracellular markers. To address this question, we stimulated exocytosis in the presence of sulforhodamine, a membrane-impermeant red fluorescent dye that is not detectable in the GFP channel of the microscope. At the end of the stimulation, sulforhodamine was washed out. As shown in Fig. 2*A*, red fluorescent spots were observed that precisely colocalized with secretory granules, with a strong preference for granules that had undergone intensity changes in the GFP channel during the preceding stimulation period (Fig. 2*A*). In addition, we observed red-labeled structures of more irregular shape that did not colocalize with green-labeled structures and that probably represent components of the endosomal pathway (not shown).

To quantify this effect, we determined the degree of colocalization as described (20). As shown in Fig. 2*B Middle*, >30% of the active granules (F_{lost}, F_{down}, and F_{up}) were labeled with sulforhodamine. In contrast, sulforhodamine was only rarely seen in F_{const} granules (4.3 ± 2.4%, n = 339 from seven membrane sheets). The proportion of endocytically active granules was lower at 100 nM free calcium but did not change between 500 nM and 50 μM. At calcium concentrations >50 μM (shaded area in Fig. 2*B*), no reliable data could be obtained because changes in GFP fluorescence were also observed on washed-out granules that were bound to the glass surface (triangles in Fig. 2*B Top*). There was no correlation between one of the release modes (F_{lost}, F_{down}, and F_{up}) and endocytic uptake (data not shown).

We also examined whether recaptured granules can undergo a second round of exocytosis. Cells were depolarized for 2 min in the presence of sulforhodamine. Immediately after stimulation, membrane sheets were prepared by sonication. Although such sheets contained both GFP- and GFP/sulforhodamine-labeled secretory granules (data not shown), we were unable to observe exocytosis beyond background levels (Fig. 1*G*), suggesting that the granules had become refractory. If cells were incubated for 30 min in culture media after the 2-min stimulation period, membrane sheets prepared thereafter still contained both GFP- and GFP/sulforhodamine-positive granule populations. When these sheets were stimulated, normal rates of exocytosis were observed (Fig. 1*G*), with no difference between single- and double-labeled granules. However, it should be noted that under these conditions it is unclear whether the sulforhodamine label is derived from recapture or membrane recycling via endosomal pathways.

Stimulus-Dependent Labeling of Secretory Granules with Fluid-Phase Markers in Intact PC12 Cells. To confirm transient exocytosis of secretory granules by an independent approach, we stimulated intact PC12 cells in the presence of the fluid-phase marker HRP

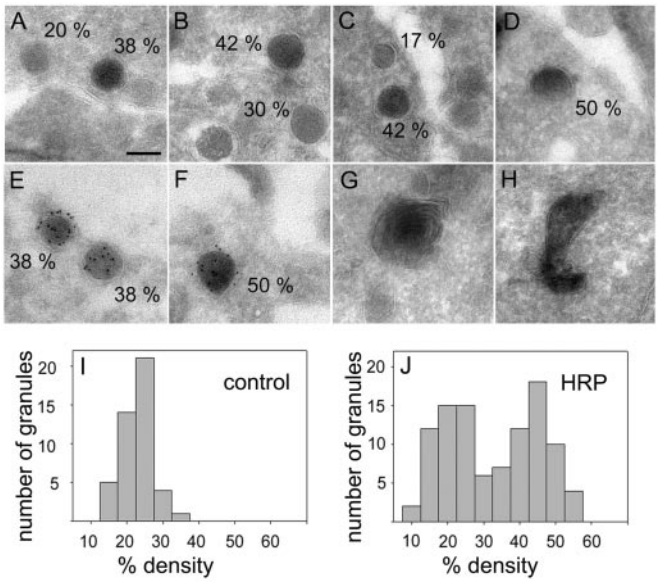

Fig. 3. Gallery of electron micrographs showing organelles sequestering HRP after 2 min of high K^+ stimulation of intact PC12 cells. Organelles that have taken up HRP appear more electron dense. To quantitate HRP uptake, line scans were performed through the center of the labeled structure, measuring its average intensity ($gran_{int}$) and the intensity of the surrounding cytosol (cyt_{int}). Secretory granules were identified because of their round shape, size (a diameter of ≈120 nm in this clone; ref. 51), and the presence of a clearly visible dense core devoid of internal membrane. The density was calculated according to: percentage density = $(1 - gran_{int}/cyt_{int}) \times 100$. (*A–D*) Organelles classified as secretory granules (numbers indicate percentage density; see text). (*E* and *F*) Double labeling of secretory granules from NPY-GFP-transfected cells containing GFP (ImmunoGold labeling) and trapped HRP after stimulation of intact cells. (*G* and *H*) HRP-labeled organelles probably representing endosomes. (Scale bar, 100 nm.) (*I* and *J*) Histograms showing the percentage density distribution of secretory granules in stimulated cells in the absence (*I*, $n = 45$ granules) and presence (*J*, $n = 101$ granules) of HRP.

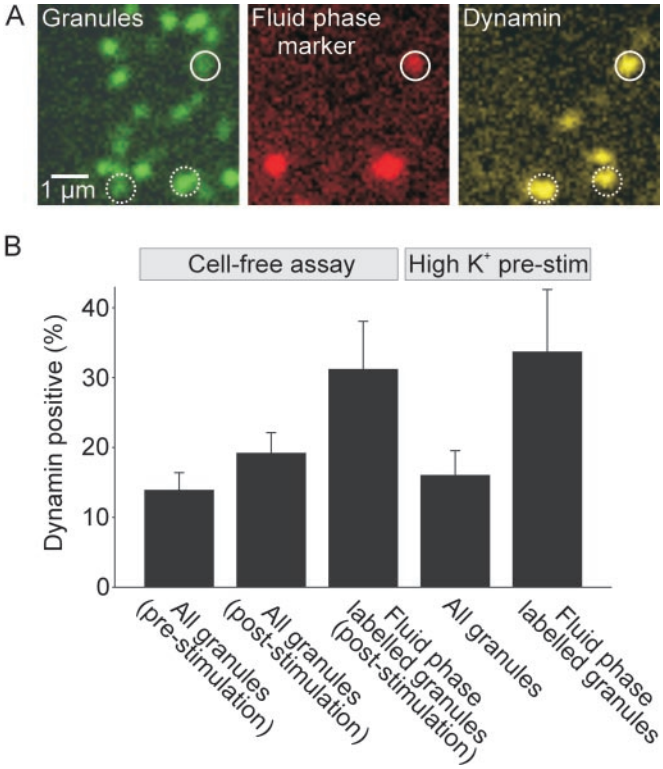

Fig. 4. Association of secretory granules with dynamin. (*A*) Triple-labeling of membrane sheets that were stimulated for exocytosis as in Fig. 1 and then fixed. The position of secretory granules was visualized by NPY-GFP (green channel). Granule recapture was monitored by sulforhodamine uptake (red channel, see Fig. 2*A*). Dynamin (far-red channel, displayed as yellow) was localized by immunocytochemistry using a standard procedure (17) except that all incubation times were shortened by ≈70%. (*B*) Percentage of granules colocalized with dynamin immunoreactivity. The first column is derived from experiments in which membrane sheets were prepared, immediately fixed, and stained for dynamin. For the second and third columns membrane sheets were prepared and stimulated for exocytosis with 0.5 μM $[Ca^{2+}]_{free}$, 2 mM MgATP, and 0.5 mg/ml rat brain cytosol in the presence of 5 μM sulforhodamine, followed by washing, fixation, immunolabeling, and imaging. The last two columns are derived from experiments in which intact PC12 cells were prestimulated by high K^+ for 2 min in the presence of 20 μM sulforhodamine. This process was immediately followed by generation of membrane sheets, fixation, and immunostaining for dynamin. In all cases association of granules with dynamin was corrected for channel crosstalk as well as for random association. For every condition 12 membrane sheets were analyzed. Values are mean ± SEM.

and then analyzed the cells by electron microscopy. As expected, labeling was observed in small, uncoated, round and elongated membrane profiles that probably represent early endosomal structures (Fig. 3 *G* and *H*; see ref. 22). However, labeling was also detected in vesicles with morphological features indistinguishable from secretory granules (Fig. 3 *A–D*), often in close proximity to the plasma membrane. To document that the high electron density of these granules is indeed a result of HRP uptake and not density variations of granule cores, we profiled the intensity distribution and compared it with secretory granules from cells that were stimulated in the absence of HRP. In the presence of HRP, two peaks of relative core densities were identified, one at ≈20%, the other at ≈45% (Fig. 3*J*). In the absence of HRP only one peak at 20% density was found (Fig. 3*I*). Nonstimulated cells processed in parallel also displayed some HRP-labeled secretory granules, but to a much lower extent (data not shown).

Despite the morphological similarity of the labeled vesicles to bona fide secretory granules, it cannot be excluded that these vesicles represent endosomal structures rather than recaptured granules retaining part of their protein cargo. We therefore performed HRP labeling of PC12 cells that were transfected with the secretory granule marker NPY-GFP. The resulting sections were then ImmunoGold-labeled for GFP by using a GFP-specific antibody. As shown in Fig. 3 *E* and *F*, we observed numerous vesicles with morphological characteristics of secretory vesicles that were labeled for both GFP and the extracellular marker. No gold label was found in untransfected cells with or without HRP labeling (data not shown).

Retrieval of Secretory Granules Depends on Dynamin Function. The results described so far suggest that under our assay conditions a sizeable portion (≈30%) of all fused secretory granules are recaptured by a spatially and temporally coupled, direct retrieval mechanism. The question then arises as to whether the molecular mechanism involved in retrieval is a reversal of fusion (as suggested in ref. 5) or whether a different and independent mechanism involves dynamin. Given the well established role of the GTPase dynamin in a variety of endocytic reactions (23–27), we examined whether this protein plays a role in vesicle recapture in our assay. Dynamin was shown to oligomerize into rings around the neck of endocytic vesicles and is thought to play a crucial function in the nanomechanics of membrane fission (28, 29). First, we examined whether dynamin is present at sites where secretory granules are attached, and, if so, whether there is a correlation between the presence of dynamin and granule recapture. Membrane sheets from cells containing GFP-labeled granules were fixed and immunostained for dynamin (Fig. 4*A*). About 12% of all granules colocalized with dynamin, with no

significant change after stimulation of exocytosis (Fig. 4*B*). However, when we determined dynamin colocalizion with granules that had sequestered fluid-phase marker during stimulation, the degree of overlap was statistically significantly higher (>30%, Fig. 4*B*). The same was true for green/red granules on membrane sheets derived from cells preloaded with sulforhodamine by depolarization-induced stimulation for 2 min (Fig. 4*B*). These numbers are probably underestimated because dynamin staining needed to be corrected for crosstalk from the sulforhodamine channel, thus reducing our sensitivity for dynamin detection. Furthermore, it is possible that dynamin dissociates from the retrieval site after fission and thus can no longer be detected at the time of fixation (30, 31).

We next tested whether addition of guanosine 5′-[γ-thio]triphosphate (GTPγS) inhibits the endocytic uptake of a fluid-phase marker in our cell-free assay. GTPγS locks dynamin in the GTP-bound state (32, 33) and prevents dynamin-dependent membrane fission (33). Indeed, GTPγS inhibited recapture of secretory granules by almost 60%, whereas hydrolyzable GTP had no effect (Fig. 2*C*). Finally, we investigated whether granule recapture is prevented by two peptides that are known to block the action of dynamin in endocytosis by interfering with interactions of its proline-rich domain. The first corresponds to residues 828–842 of dynamin (34). The second is the GST-fusion protein of the Src homology 3 (SH3) domain of amphiphysin (18). A strong inhibition of granule recapture was observed with the dynamin peptide that was almost complete at the maximal concentration (Fig. 2*D*). Addition of 50 μM of the amphiphysin SH3 domain caused a similarly strong inhibition, whereas GST alone had no effect (Fig. 2*D*). No significant change in rates of exocytosis was observed in the presence of any of the peptides or the guanine nucleotides (data not shown) in agreement with the recent findings of Graham *et al.* (14). Together the data suggest that retrieval of secretory granules by recapture depends on dynamin.

Discussion

The presence of amperometric "foot" signals suggested that exocytosis of dense core secretory granules is preceded by the opening of a fusion pore that may remain arrested for some time before expanding (35, 36) and that occasionally may reclose (37). Using PC12 cells as a model for a neuroendocrine cell, we have now shown that up to one-third of all secretory granules undergoing stimulus-dependent exocytosis are recaptured at the site of exocytosis without undergoing full fusion. Recapture was observed in surface-attached membrane sheets but confirmed in intact cells. Furthermore, recapture depends on dynamin. These findings complement with morphological evidence a recent study by Graham *et al.* (14), who have used amperometric methods to monitor the opening time of putative exocytotic fusion pores.

The requirement of dynamin for granule recapture, at least for a significant subpopulation of such events, provides firm evidence that the molecular mechanisms of exocytosis and endocytosis are different even in a case where the two reactions are very tightly coupled. Exocytosis requires soluble *N*-ethylmaleimide-sensitive factor attachment protein receptors (SNAREs) to convert from "trans" to "cis" complexes, a reaction that is thought to drive membrane merger. SNARE assembly follows a steep energy gradient and is essentially irreversible (38). Disassembly requires the efforts of the chaperone-like ATPase *N*-ethylmaleimide-sensitive factor and is presumably a relatively slow reaction (39). Dynamin is thought to provide either directly (33, 40, 29) or indirectly (30) a mechanical force needed to sever the tubular membrane of the vesicle neck, in our case the neck generated by the fusion pore. Our data suggest that dynamin assembles at sites of release before the granule fuses and may thus be in place for mediating recapture as soon as exocytosis occurs.

Dynamin belongs to a family of GTPases that are involved both in membrane fission and signaling events (28, 41). Although dynamin is best characterized for its crucial role in the pinching off of clathrin-coated vesicles, it has also been implicated in other types of endocytosis, including caveolin-dependent endocytosis and fluid-phase endocytosis (24–27, 42). Thus, it is not surprising to find a role of dynamin in an endocytic recapture reaction (this study and ref. 14) that does not appear to depend on clathrin, although a possible role of clathrin in the recapture mechanism described by us cannot be completely excluded without further investigations. Irrespective of the mechanism of fission and the number of factors involved, our findings (together with the recent study of ref. 14; see also refs. 23 and 43) agree with the concept that fusion and fission are unidirectional, irreversible reactions.

The sequence of reaction described here fits a broad definition of "kiss-and-run" exo–endocytosis, but may not necessarily apply to the exo–endocytosis of classical neurotransmitter-containing synaptic vesicles. The classical kiss-and-run model was originally developed for such vesicles to explain their fast recycling rate and the reported lack of correlation between exocytosis and the appearance of clathrin-coated vesicles in nerve terminals (4, 44). A kiss-and-run fusion of synaptic vesicles received further support from endocytic tracers uptake and release studies at synapses (45, 46). These studies suggested an exocytotic opening too short for a complete equilibration of the tracers between the lumen of the vesicle and the extracellular media (46–48). Because of the fast diffusion rate of the tracers used, these results imply opening and closure of fusion pores in the submillisecond range and thus a time scale (ms range) much faster than the dense core granule recapture reaction analyzed in our study.

Several previous studies dealt with the endocytic pathway in neuroendocrine cells, including PC12 cells. In a recent study by de Wit *et al*. (22), the progression of endocytic markers through various organelles has been analyzed by quantitative electron microscopy using BSA with bound nanogold particles as tracer. Early endocytic structures including coated vesicles, small round vesicles, and elongated cisternae were observed that were also seen in our analysis, but apparently no evidence for labeling of secretory granules was obtained. In this study, however, uptake was performed under nonstimulating conditions. It is also possible that BSA-gold is too large to enter the granule during transient fusion, or it is prevented from uptake by the flow of ongoing protein discharge, which would be less of a problem for smaller molecules with a higher diffusivity. Interestingly, recapture of secretory granules was postulated many years ago based on an electron microscopic analysis of organelles labeled with extracellular tracers (49), and stimulus-dependent labeling of secretory granules with an endocytic tracer has also been observed in a more recent study (50). Like in the capacitance experiments, however, it was not possible to spatially correlate exocytosis with endocytosis in such approaches.

We are indebted to Drs. Wolfhard Almers and Erwin Neher for critical discussions during the course of the project and Dr. Irina Majoul for the kind gift of GFP antibody. This work was supported in part by funds from the Gottfried Wilhelm Leibniz Program of the Deutsche Forschungsgemeinschaft (to R.J.).

1. Huttner, W. B., Ohashi, M., Kehlenbach, R. H., Barr, F. A., Bauerfeind, R., Braunling, O., Corbeil, D., Hannah, M., Pasolli, H. A., Schmidt, A., *et al*. (1995) *Cold Spring Harbor Symp. Quant. Biol.* **60,** 315–327.
2. Burgess, T. L. & Kelly, R. B. (1987) *Annu. Rev. Cell Biol.* **3,** 243–293.
3. Heuser, J. E. & Reese, T. S. (1973) *J. Cell Biol.* **57,** 315–344.
4. Ceccarelli, B. & Hurlbut, W. P. (1980) *Physiol. Rev.* **60,** 396–441.
5. Fesce, R. & Meldolesi, J. (1999) *Nat. Cell Biol.* **1,** E3–E4.
6. Lindau, M. & Almers, W. (1995) *Curr. Opin. Cell Biol.* **7,** 509–517.
7. Artalejo, C. R., Elhamdani, A. & Palfrey, H. C. (1998) *Curr. Biol.* **8,** R62–R65.

8. Alvarez de Toledo, G., Fernandez-Chacon, R. & Fernandez, J. M. (1993) *Nature* **363,** 554–558.
9. Albillos, A., Dernick, G., Horstmann, H., Almers, W., Alvarez de Toledo, G. & Lindau, M. (1997) *Nature* **389,** 509–512.
10. Ales, E., Tabares, L., Poyato, J. M., Valero, V., Lindau, M. & Alvarez de Toledo, G. (1999) *Nat. Cell Biol.* **1,** 40–44.
11. Jahn, R. & Sudhof, T. C. (1999) *Annu. Rev. Biochem.* **68,** 863–911.
12. Chen, Y. A. & Scheller, R. H. (2001) *Nat. Rev. Mol. Cell Biol.* **2,** 98–106.
13. Slepnev, V. I. & De Camilli, P. (2000) *Nat. Rev. Neurosci.* **1,** 161–172.
14. Graham, M. E., O'Callaghan, D. W., McMahon, H. T. & Burgoyne, R. D. (2002) *Proc. Natl. Acad. Sci. USA* **99,** 7124–7129.
15. Heumann, R., Kachel, V. & Thoenen, H. (1983) *Exp. Cell Res.* **145,** 179–190.
16. Lang, T., Wacker, I., Steyer, J., Kaether, C., Wunderlich, I., Soldati, T., Gerdes, H. H. & Almers, W. (1997) *Neuron* **18,** 857–863.
17. Lang, T., Bruns, D., Wenzel, D., Riedel, D., Holroyd, P., Thiele, C. & Jahn, R. (2001) *EMBO J.* **20,** 2202–2213.
18. Grabs, D., Slepnev, V. I., Songyang, Z., David, C., Lynch, M., Cantley, L. C. & De Camilli, P. (1997) *J. Biol. Chem.* **272,** 13419–13425.
19. Avery, J., Ellis, D. J., Lang, T., Holroyd, P., Riedel, D., Henderson, R. M., Edwardson, J. M. & Jahn, R. (2000) *J. Cell Biol.* **148,** 317–324.
20. Lang, T., Margittai, M., Holzler, H. & Jahn, R. (2002) *J. Cell Biol.* **158,** 751–760.
21. Patterson, G. H., Knobel, S. M., Sharif, W. D., Kain, S. R. & Piston, D. W. (1997) *Biophys. J.* **73,** 2782–2790.
22. de Wit, H., Lichtenstein, Y., Geuze, H. J., Kelly, R. B., van der Sluijs, P. & Klumperman, J. (1999) *Mol. Biol. Cell* **10,** 4163–4176.
23. Artalejo, C. R., Lemmon, M. A., Schlessinger, J. & Palfrey, H. C. (1997) *EMBO J.* **16,** 1565–1574.
24. Henley, J. R., Krueger, E. W., Oswald, B. J. & McNiven, M. A. (1998) *J. Cell Biol.* **141,** 85–99.
25. Oh, P., McIntosh, D. P. & Schnitzer, J. E. (1998) *J. Cell Biol.* **141,** 101–114.
26. Lee, E. & De Camilli, P. (2002) *Proc. Natl. Acad. Sci. USA* **99,** 161–166.
27. Orth, J. D., Krueger, E. W., Cao, H. & McNiven, M. A. (2002) *Proc. Natl. Acad. Sci. USA* **99,** 167–172.
28. Danino, D. & Hinshaw, J. E. (2001) *Curr. Opin. Cell Biol.* **13,** 454–460.
29. Marks, B., Stowell, M. H., Vallis, Y., Mills, I. G., Gibson, A., Hopkins, C. R. & McMahon, H. T. (2001) *Nature* **410,** 231–235.
30. Sever, S., Damke, H. & Schmid, S. L. (2000) *J. Cell Biol.* **150,** 1137–1148.
31. Tsuboi, T., Terakawa, S., Scalettar, B. A., Fantus, C., Roder, J. & Jeromin, A. (2002) *J. Biol. Chem.* **277,** 15957–15961.
32. Stowell, M. H., Marks, B., Wigge, P. & McMahon, H. T. (1999) *Nat. Cell Biol.* **1,** 27–32.
33. Takei, K., McPherson, P. S., Schmid, S. L. & De Camilli, P. (1995) *Nature* **374,** 186–190.
34. Shupliakov, O., Low, P., Grabs, D., Gad, H., Chen, H., David, C., Takei, K., De Camilli, P. & Brodin, L. (1997) *Science* **276,** 259–263.
35. Chow, R. H., von Ruden, L. & Neher, E. (1992) *Nature* **356,** 60–63.
36. Neher, E. (1993) *Nature* **363,** 497–498.
37. Bruns, D. & Jahn, R. (1995) *Nature* **377,** 62–65.
38. Fasshauer, D., Antonin, W., Subramaniam, V. & Jahn, R. (2002) *Nat. Struct. Biol.* **14,** 144–151.
39. Morgan, A., Dimaline, R. & Burgoyne, R. D. (1994) *J. Biol. Chem.* **269,** 29347–29350.
40. Sweitzer, S. M. & Hinshaw, J. E. (1998) *Cell* **93,** 1021–1029.
41. Di Fiore, P. P. & De Camilli, P. (2001) *Cell* **106,** 1–4.
42. Artalejo, C. R., Henley, J. R., McNiven, M. A. & Palfrey, H. C. (1995) *Proc. Natl. Acad. Sci. USA* **92,** 8328–8332.
43. Artalejo, C. R., Elhamdani, A. & Palfrey, H. C. (2002) *Proc. Natl. Acad. Sci. USA* **99,** 6358–6363.
44. Heuser, J. (1989) *Cell Biol. Int. Rep.* **13,** 1063–1076.
45. Klingauf, J., Kavalali, E. T. & Tsien, R. W. (1998) *Nature* **394,** 581–585.
46. Stevens, C. F. & Williams, J. H. (2000) *Proc. Natl. Acad. Sci. USA* **97,** 12828–12833.
47. Kavalali, E. T., Klingauf, J. & Tsien, R. W. (1999) *Proc. Natl. Acad. Sci. USA* **96,** 12893–12900.
48. Zakharenko, S. S., Zablow, L. & Siegelbaum, S. A. (2002) *Neuron* **35,** 1099–1110.
49. Sawano, F., Ravazzola, M., Amherdt, M., Perrelet, A. & Orci, L. (1986) *Exp. Cell Res.* **164,** 174–182.
50. Henkel, A. W., Horstmann, H. & Henkel, M. K. (2001) *FEBS Lett.* **505,** 414–418.
51. Tooze, S. A., Flatmark, T., Tooze, J. & Huttner, W. B. (1991) *J. Cell Biol.* **115,** 1491–1503.